HHS Public Access

Author manuscript

Nature. Author manuscript; available in PMC 2018 October 04.

Published in final edited form as:

Nature. 2018 April ; 556(7700): 239–243. doi:10.1038/s41586-018-0016-3.

Advanced maturation of human cardiac tissue grown from pluripotent stem cells

Kacey Ronaldson-Bouchard[1], **Stephen P. Ma**[1], **Keith Yeager**[1], **Timothy Chen**[1], **LouJin Song**[2], **Dario Sirabella**[1], **Kumi Morikawa**[2], **Diogo Teles**[1,3,4], **Masayuki Yazawa**[2], and **Gordana Vunjak-Novakovic**[1,5,*]

[1]Laboratory for Stem Cells and Tissue Engineering, Department of Biomedical Engineering, Columbia University, New York, NY

[2]Department of Rehabilitation and Regenerative Medicine, Department of Pharmacology, College of Physicians and Surgeons, Columbia University, New York, NY

[3]Life and Health Sciences Research Institute (ICVS), School of Medicine, University of Minho, Braga, Portugal

[4]ICVS/3B's, PT Government Associate Laboratory, Braga/Guimarães, Portugal

[5]Department of Medicine, Columbia University, New York, NY

Abstract

Cardiac tissues generated from human induced pluripotent stem (iPS) cells can serve as platforms for patient-specific studies of physiology and disease[1–6]. The predictive power of these models remains limited by their immature state[1,2,5,6]. We show that this fundamental limitation could be overcome if cardiac tissues are formed from early iPS-derived cardiomyocytes (iPS-CM), soon after the initiation of spontaneous contractions, and subjected to physical conditioning of an increasing intensity. After only 4 weeks of culture, these tissues displayed adult-like gene expression profiles, remarkably organized ultrastructure, physiologic sarcomere length (2.2 μm) and density of mitochondria (30%), the presence of transverse tubules (t-tubules), oxidative metabolism, positive force-frequency relationship, and functional calcium handling for all iPS cell

*Please address correspondence to: Gordana Vunjak-Novakovic, Columbia University, 622 West 168th Street, VC12-234, New York NY 10032, Tel: 212 305 2304; gv2131@columbia.edu.
Correspondence and requests for materials should be addressed to G.V.N. (gv2131@columbia.edu).

Extended data are linked to the online version of the paper at www.nature.com/nature

Author contributions: KRB and GVN designed the study; KRB, KY and GVN designed the tissue culture platform; KRB, SPM, TC and DT conducted cultivations of all types of tissues at different stimulation regimens, and the real-time and end-point assessments of tissue properties (including gene expression, histomorphology, ultrastructure, distributions of cardiac proteins, contractile behavior, and calcium handling). KRB, SPM, TC and DT were able to replicate the entire process of tissue cultivation and assessment, independently. DS and LS expanded iPS cells and derived cardiomyocytes. KRB conducted immunostains for the presence of t-tubules. MY, KM and LS conducted single cell dissociation and electrophysiology. KRB, SPM, TC, MY and GVN interpreted data and wrote the manuscript.

The authors declare the following competing financial interests: GVN and KRB are cofounders of TARA Biosystems, a Columbia spinout commercializing the use of bioengineered human cardiac tissue for drug testing.

Readers are welcome to comment on the online version of the paper.

lines studied. Electromechanical properties developed more slowly and did not achieve the stage of maturity seen in adult human myocardium. Tissue maturity was necessary for achieving physiologic responses to isoproterenol and recapitulating pathological hypertrophy, in support of the utility of this tissue model for studies of cardiac development and disease.

Even our best methods have limited ability to emulate the physiology of adult myocardium[1–11,31], with the excitation-contraction coupling (requiring t-tubules), positive force frequency relationship (requiring mature calcium handling), and efficient energy conversion (requiring oxidative metabolism) notably absent[2–3,5,6,8–10]. Adult ventricular myocytes are uniquely organized for beating function, with densely packed sarcomeres, mitochondria, t-tubules, and sarcoplasmic/endoplasmic reticulum (SR/ER). The mitochondria are positioned adjacent to sarcomeres and calcium pumps to enhance ATP diffusion; the SR provides fast delivery of stored calcium ions to contractile proteins; the t-tubules synchronize heartbeats by concentrating L-type calcium channels, positioned close to ryanodine receptors releasing calcium ions from SR/ER[12]. This highly specialized machinery for excitation–contraction coupling is not observed in fetal heart, but emerges after birth[13], with the switch from glycolytic to oxidative metabolism supporting energy demands of postnatal heart[14].

Human iPS-CMs can be matured by long-term culture, electrical, hydrodynamic and mechanical stimulation[8,9,15–17,31]. Recent studies indicate that the *in vitro* culture may not follow the developmental paradigm: high stimulation frequencies benefit maturation *in vitro*[9], while the native heart beats more slowly following birth[5,13]. We asked why current strategies stop short of achieving the hallmarks of adult myocardium. Because the responsiveness of iPS-CM to physical stimuli declines with the progression of differentiation, we hypothesized that electromechanical conditioning should be initiated early, during the period of high cell plasticity. Since the heart matures in response to energy demands, we further hypothesized that the increasing intensity of induced contractions will enhance the development of mature ultrastructure and function.

To test these hypotheses, we studied maturation of human cardiac tissues grown from: (*i*) *early-stage* iPS-CMs (day 12, immediately following the first spontaneous contractions) and (*ii*) *late-stage* iPS-CMs (day 28, matured in culture). Cardiac tissues were assembled in a modular tissue platform enabling individual control of culture environment and physical signaling. Human iPS-CMs (derived from three donors) and supporting fibroblasts were incorporated into fibrin hydrogel stretched between two flexible pillars (designed to provide mechanical forces similar to those in native myocardium), and subjected to electrical stimulation to induce auxotonic contractions. Three conditioning regimes were applied: (*i*) *control* (no stimulation), (*ii*) *constant* (3 weeks at 2 Hz), and (*iii*) *intensity training* (2 weeks at a frequency increasing from 2 to 6 Hz by 0.33 Hz/day, followed by 1 week at 2 Hz; *early/intensity* and *late/intensity* tissues). The resulting tissues measured 6 mm long and 1.8 mm in diameter, and were evaluated in real-time (contractile and conductive behavior, calcium handling) and by end-point assays (genes, proteins, ultrastructure), using human fetal cardiac tissues (FCTs) and adult human heart ventricles as benchmarks (Fig. 1a, Extended data Fig. 1a–e). *Early/intensity* tissues displayed compact and well differentiated cardiac

muscle (Extended data Fig. 1f–n), and comprehensive changes in genes encoding for adult-like conduction (↑ITPR3, ↑KCNH2, ↓HCN4), maturation (↑NPPB, ↑MAPK1, ↑PRKACA), ultrastructure (↑β-myosins, ↑Cx-43, ↑TNNI3, ↑AKAP6, ↑GJA5, ↑JPH2), energetics (↑PRKA1, ↑TFAM, ↑PPARGC1A), and calcium handling (↑CAV3, ↑BIN1, ↑ATP2A2, ↑RYR2, ↑ITPR3); the other early-stage tissues, all late-stage tissues, and FCTs displayed immature cardiac phenotypes (Fig. 1b, Extended data Fig. 2a,b).

The formation of cardiac tissues from early iPS-CMs was critical for their response to physical signals. Only the *early/intensity* tissues displayed orderly signal propagation and anisotropic gap junctions. Among all groups, *early/intensity* tissues had superior electrophysiological properties that were comparable to Biowires[9], including the action potential shape with a characteristic notch, resting membrane potential of −70 ± 2.7 mV, the I_{K1} current (peak inward density of −9.9 ± 3.8 pA/pF; peak outward density of 0.30 ± 0.12 pA/pF), and the conduction velocity (25 ± 0.9 cm/s) (Fig. 1c–d, Extended data Fig. 2 and Fig. 3a–f, Supplementary Videos 1,2).

Early/intensity tissues displayed a positive force-frequency relationship (FFR), a hallmark of maturation not previously achieved[5,6]. The generated forces markedly exceeded those in all other groups and fetal tissues (Fig. 1f), but remained below those in adult myocardium (44 mN/mm^2)[19]. Directly measured forces and amplitudes of contraction increased approximately two-fold over the range of stimulation frequencies (1–6 Hz) indicating the maturation of contractile behavior in *early/intensity* tissues. These tissues acquired regular contraction profiles, in contrast to late-stage tissues (Extended data Fig. 3g–i and Fig. 4a–d, Supplementary Movies 1, 2). The surrogate measurements of force from calcium recordings in early/intensity tissues (Extended data Fig. 3j–k), were consistent with the direct force measurements.

Cell populations were dominated by cardiomyocytes, and the $MLC2v^+/MLC2a^+$ ratio depended on stimulation regime and developmental stage of iPS-CMs. The increasing contractile demands induced adult-like cardiac morphology for high force generation in *early/intensity* tissues. The cell size increased (an indicator of physiological hypertrophy[8]) and both the cells and nuclei elongated (an indicator of maturation[8]). The sarcomere length reached 2.2 μm, a value measured for adult human ventricular myocytes[8]. The contractile capacity, fraction of cells containing sarcomeres, and the organization of sarcomeric α-actinin resembled that in adult human myocardium (Fig. 1e, Extended Data Fig. 4e–k and Fig. 5).

Ultrastructural development was also determined by the developmental stage of iPS-CMs and the stimulation regime. Only *early/intensity* tissues displayed orderly registers of sarcomeres with I/A-bands, M-lines, Z-lines, desmosomes, intercalated discs, a high density of mitochondria positioned adjacent to the contractile machinery and proteins organized for increased energetics (Fig. 2a–b, Extended data Fig. 6 and 7a–b).

While fetal heart favors glucose as the primary energy substrate[19], increased workload in the postnatal heart leads to matured mitochondria optimized for fatty acid oxidation[21,22]. The percent area of mitochondria in early/intensity tissues (30± 2.9 %) was at the levels

measured for adult human myocardium[20,24]. Active biogenesis[23] was associated with the production of phospholipids near the sarcomeres, a switch to oxidative metabolism, and the formation of t-tubules (Fig. 2c–f, Extended data Fig. 7c–d).

Early/intensity tissues contained robust t-tubules seen both longitudinally and in cross sections. T-tubules (WGA, di-8-anepps) were co-localized with the bridging integrator 1 (BIN1), ryanodine receptor 2 (RyR2), and L-type calcium channels ($Ca_V1.2$/*CACNA1C*) at the spacing optimized for calcium handling (Fig. 2g–k, Extended data Fig. 8), as in adult heart[29]. These tissues displayed spatially uniform cell density, presumably due to the enhanced transport of nutrients and metabolites during tissue contractions, generated the highest force, and expressed the CICR modulators RYR2 (SR/ER calcium release) and BIN1 (control of ion flux along t-tubules[26]) (Fig. 3a, Extended data Fig. 8a,f,g and Fig. 9a).

The frequency-dependent acceleration of relaxation (FDAR), an intrinsic property of adult myocardium that was observed for *early/intensity* tissues showed that the tissues subjected to supra-threshold electrical pacing regimens developed mechanisms to respond to the increasing workload. The ultrastructural machinery for contraction/relaxation was confirmed by the positioning of t-tubules in proximity to cardiac calcium pump SERCA2A/*ATP2A2* and sodium-calcium exchanger NCX1/*SLC8A1*. Consistently, transcription of the genes responsible for clearing cytosolic calcium (*ATP2A2* and *SLC8A1*[17]) increased over time and the sequestration and extrusion of calcium became faster, enabling the iPS-CMs to relax and respond to contractile triggers. Blocking $Ca_V1.2$ by nifedipine or verapamil gradually reduced calcium transients in a training-dependent manner, while the response to caffeine indicated that only the *early/intensity* tissues had functional intracellular calcium stores. Blocking SERCA by thapsigargin to prevent SR/ER calcium uptake halted calcium transients, indicating dependence on functional SR. The subsequent addition of caffeine had no effect, consistent with calcium depletion of the SR/ER (Fig. 3b–d, Extended data Fig. 9b–h).

Post-rest potentiation confirmed functionality of SR/ER calcium stores in *early/intensity* tissues. All other tissues failed to respond to increased calcium levels and developed calcium alternans, due to the lack of t-tubules and inefficient coupling between intracellular calcium entry and release. When CICR was blocked with ryanodine to test the RyR2 function, only *early/intensity* tissues showed response, likely due to the presence of t-tubules in this group, which are critical for proper CICR. Importantly, the positive FFR was blunted upon blocking RyR2 by ryanodine and completely reversed upon using thapsigargin to block calcium storage by SERCA2a, indicating the importance of both CICR and the reuptake of calcium into the SR (Fig. 3e, Extended data Fig. 9i–k).

Because a functional β-adrenergic receptor system is dependent on both intracellular calcium reserves and the proximity of $Ca_V1.2$ channels and t-tubules[4,26,27], comprehensive responses to β-adrenergic agonists are an indicator of phenotypic maturation[28]. We examined if *early/intensity* tissues had ability for ionotropic response to isoproterenol, since current efforts to capture this effect have been unsuccessful[2,10]. Indeed, we measured positive chronotropic, ionotropic, and lusitropic responses to isoproterenol, with EC_{50} values corresponding to those in clinical studies[18] (Fig. 3f–h, Extended data Fig. 10a–b).

Tissue maturity was necessary for recapitulating critical aspects of cardiac hypertrophy (HCM), a leading cause of sudden cardiac death in athletes[2]. As expected, hypertrophic tissues displayed decreased beating frequency, increased intracellular calcium transient durations and decay times relative to healthy controls, and were not able to capture at high frequencies. The onset of HCM diminished the FDAR and resulted in a negative FFR, in contrast to healthy tissues. Differences between healthy and diseased groups were most pronounced in the intensity-stimulated tissues (Fig. 3i–j, Extended data Fig. 10c–f).

A recent study[31] reported large (7x7 mm to 36x36 mm) and thin (50μm) human heart tissues grown without exogenous stimulation that displayed less developed ultrastructure, no evidence of oxidative metabolism, slightly negative FFR, comparable APD and conduction velocity, and approximately 4-fold higher force per unit cross-sectional tissue area. It would be instructive to explore how the different tissue geometries (very thin patches vs. cylindrical muscle) and culture protocols (no external stimulation vs. intensity training) between that[31] and this current study contributed to the measured structural and functional tissue outcomes.

In summary, we demonstrate that adult-like human cardiac tissue can be grown from iPS-CMs in fibrin hydrogel subjected to stretch and auxotonic contractions, over just 4 weeks of *in vitro* culture. Two methodological advances enabled accelerated cardiac maturation: the formation of tissues from *early-stage iPS-CMs* (that displayed significant plasticity), immediately after the initiation of spontaneous contractions, and *physical conditioning at an increasing intensity* (that mimicked mechanical loading during the fetal-postnatal transition). Under these conditions, tissues developed unprecedented adult-like gene expression and tissue ultrastructure throughout the tissue volume, oxidative metabolism, FDAR, positive FFR, and physiologic calcium handling.

An important result of our study is that the highly accelerated and rather complete maturation of the molecular, structural and metabolic features was associated with a slower and less complete establishment of mature cardiac function. We demonstrate that physiological cell density was not sufficient to achieve adult mechanical function; that the FDAR and positive FFR can be established at subnormal levels of force generation; and that t-tubules and oxidative metabolism are required for physiological FFR and calcium handling. Two factors could contribute to the contrast between impressive morphological maturation and the less complete functional maturation: our tissue model does not recapitulate the macroscopic structure of myocardium, and the period of 4 weeks may be too short for establishing all functional features. It is therefore of interest to use this human cardiac tissue model to study the progression of functional maturation.

METHODS

Cardiac differentiation of human iPS cells

Human induced pluripotent stem cells (hiPSC) were obtained through Material Transfer Agreements from Stephen Duncan, University of Wisconsin (C2A line), Bruce Conklin, Gladstone Institute (WT11 line) and Masayuki Yazawa, Columbia University (IMR90 line). hiPSCs were expanded on growth factor reduced Matrigel-coated plates (Corning) in mTeSR1 media (Stemcell technologies) that was changed on a daily basis, and passaged

upon reaching 85–95% confluence at a 1:6 split ratio utilizing Accutase (Life Technologies). During the first 24 hours after passaging, 5 μM Y-27632 dihydrochloride (Tocris, 1254) was supplemented to culture medium.

Cardiac differentiation of iPSCs was initiated in confluent monolayers by replacing the mTeSR1media with RPMI+B27-insulin media, consisting of RPMI-1640 (Life Technologies), 1x B27 supplement without insulin (a source of omega-3 fatty acids and also of the thyroid hormone that promotes cardiac maturation, Life Technologies), 100 U penicillin (Life Technologies), 0.1 mg/mL streptomycin (Life Technologies), 50 μg/mL ascorbic acid (Sigma, A4544). During the first 24 hours, the medium was further supplemented with activin A (50 ng/mL, R&D Systems) and bone morphogenetic protein 4 (BMP4, 25 ng/mL, R&D systems). From 24 – 72 hrs, the RPMI+B27-insulin media were supplemented with vascular endothelial growth factor (10 ng/mL VEGF, R&D systems). Beyond 72 hours, through the end of differentiation process (up to 12 days), RPMI+B27 media consisting of RPMI-1640, 1x B27 supplement with insulin (Life Technologies), 100 U penicillin, 0.1 mg/mL streptomycin, and 50 μg/mL ascorbic acid, was used and refreshed every 2 days. At day 12, the cells were characterized by flow cytometry using the cardiomyocyte-specific marker cTnT (clone 13–11, NeoMarkers). Differentiation typically resulted in cell populations containing 80–90% cTnT-positive cells at day 12, which were subsequently used in experiments without selection for cardiomyocytes.

Human fetal cardiac tissues

Fetal hearts were purchased as surgical waste from Advanced Bioscience Resources (Alameda, CA), and delivered on ice within 2.5 hours of surgery. Left ventricles were sectioned from the apex towards the atria into 7mm long x 2mm wide strips, washed 3 times in Hanks Balanced Salt Solution (Gibco), transferred to low attachment 6-well plates (Nunc) containing RPMI+B27 media, and placed into the incubator for 1 hour before taking measurements. FCT strips were analyzed in a similar manner to the cardiac tissues for contractile behavior, force generation, gene expression, cardiac proteins, ultrastructure and histomorphology, as detailed below. In addition, RNA isolated from 32 pooled fetal hearts, ages 21–37 weeks, was obtained from Clontech (Mountain View, CA) for gene expression studies.

Human adult heart tissue

Commercially available adult heart cDNA was purchased for gene expression data (Clontech, 637213 and 3H Biomedical AB, SC6214). Tissue samples from adult left heart ventricles were obtained as surgical waste through an IRB at Columbia University.

Tissue bioreactor platform

The platform was assembled from two separate components: the wells for tissue culture, and an array of support structures with integrated elastomeric pillars for tissue attachment (1mm in diameter, 6mm axis-to-axis distance). Both components were fabricated out of polycarbonate (PC) utilizing a Computer Numerical Control (CNC) milling machine with mating features for stability and repeatable positioning (Extended Data Fig 1a–c).

The pillars were formed by centrifugal casting of polydimethylsiloxane (PDMS, Dow Corning Sylgard 184) through, and extending from, the PC support structures. The supports were first inserted into Delrin (polyoxymethylene) molds fabricated by CNC machining and PDMS (10:1 ratio PDMS to curing agent) was centrifugally cast at 400 RCF for 5 minutes and cured in an oven at 60°C for 1 hr. The resulting component consisted of three pairs of pillars to support the formation of three tissues (Extended Data Fig. 1d). Pillars were 1mm in diameter, 9mm in length, and spaced 6mm axis-to-axis.

The platform contained 12 wells for tissue culture that were patterned with the exact 48-well plate spacing, such that the platform corresponded to one quarter of the standard 48-well plate. Each well had a bottom portion measuring 10mm x 4mm x 4mm where the cells in hydrogel were introduced, and a wider top portion measuring 10mm x 7mm x 4mm for culture media. A glass slide was bonded to the bottom of the platform to allow facile microscopic observation.

Electrical stimulation of the cell-hydrogel tissues was provided via carbon rods (Ladd Research Industries) that served as electrodes. The carbon rods were placed into slots machined on each side of the culture well, aligned in parallel and positioned perpendicular to the long axis of both the culture well and the tissue. The electrodes were connected to a cardiac stimulator (Grass s88x) via platinum wires (Ladd Research Industries). Electrical stimulation was generated by a spatially uniform, pulsatile electrical field (4.5mV intensity, 2ms in duration, monophasic square waveform) perpendicular to the long axis of the tissue. The parameter settings: amplitude, duration, frequency, and waveform were controlled by the Grass s88x cardiac stimulator.

Culture of cardiac tissues

The differentiated iPS-CMs were combined with supporting human dermal fibroblasts (Lonza), cultured in Dulbecco's Modified Eagle Medium supplemented with 10% v/v fetal bovine serum, 100 U penicillin, and 0.1 mg/mL streptomycin, at a ratio of 75% iPS-CMs and 25% fibroblasts. The cells were subsequently encapsulated in fibrin hydrogel by mixing 20 mg/mL human fibrinogen (Sigma), 100U/mL human thrombin (Sigma-Aldrich), and the cell suspension at a 3:1:1 ratio. The hydrogel solution (200 μL containing 2 million cells) was dispensed into each well of the platform and allowed to polymerize at 37°C for 30 minutes, so that the tissues readily formed around the pillars. Then, 800 μL of RPMI+B27 media containing 0.2mg/mL aprotinin (Sigma-Aldrich, A3428) were added into each well, with an additional 30 mL of RPMI+B27 media containing 0.2mg/mL aprotinin (Sigma-Aldrich, A3428) added to a 100mm petri dish (Corning, 430591) containing one platform (12 tissues). Subsequent media changes occurred every other day and consisted of 30 mL of RPMI+B27 media containing 0.2mg/mL aprotinin (Sigma-Aldrich, A3428) for the first 7 days, and 30 mL of RPMI+B27 media (either day 7–28 or day 7–84).

The pillars were designed to subject the tissues to mechanical loading designed to mimic that in native human myocardium. Hydrogel compaction caused passive tension in the tissues as they were stretched between the two pillars, inducing elongation and alignment. Synchronous contractions induced by electrical stimulation generated dynamic forces in the contracting tissues attached to the pillars that were forced to work against the load.

Electrical stimulation was initiated on day 7, using one of three training regimens (Fig. 1a): *control* (no electrical stimulation, 0 Hz), *constant* (constant frequency of 2 Hz), and *intensity training* (a ramped stimulation that increased the frequency from 2 Hz at day 7 to 6 Hz at day 21, by 0.33 Hz per day; tissues were then stimulated at 2 Hz until day 28) (Extended Data Fig. 1e). Tissues were cultured for a period of 4 weeks, in 16 independent experiments that used three separate lines of hiPSCs. Detailed samples sizes for the Main Figures can be found in the Supplemental Information Main Figure Data Sample Sizes.

Tissue properties were evaluated using real-time assessment of: amplitude and frequency of contractions, calcium handling, force generation, excitation threshold, and maximum capture rate. The corresponding endpoint assays were conducted to determine cell and tissue morphology (histologically), ultrastructure (by transmission electron microscopy), gene expression (real-time qPCR), and the presence and distribution of cardiac proteins (immunohistochemistry).

Contractility analysis

Tissue contractility was measured by tracking the change in tissue area as a function of time. Live cell, bright field videos were acquired at rates of up to 150 frames per second using a Pike F-032b (Allied Vision Technologies) camera controlled with custom SPLASSH software[29]. Acquired video frames were inverted and an automated intensity threshold was used to identify cell location in the video frame. First, a baseline timepoint in the video corresponding to a relaxed tissue state was selected. Absolute differences in cell area from the baseline frame were then calculated to create a timecourse of cell area dynamics as a function of time. The resulting timecourses were analyzed using a native MATLAB automated peak finding algorithm to determine locations of maximum cell contraction indicated by the locations of local maxima in the timecourses. Beat period lengths were determined from the length of time between the pairs of local maxima. Beat frequencies were determined by inverting beat periods. Contraction amplitude relaxation times were measured from the length of time required for the tissue to relax from the peak contraction amplitude of the local maxima to the calculated relaxation amplitude (e.g., the R90 time was the length of time elapsed from the local maxima until the contraction time course reached 10% of the local maxima's contraction difference).

Calcium handling

Tissues within culture platforms were loaded with Fluo-4 NW (50% v/v, Life Technologies) in RPMI+B27 media containing 5 μM blebbistatin (Sigma) as necessary to reduce movement artifacts for 30 minutes at 37°C. Videos were acquired at a rate of 150 frames per second using a Pike F-032 camera (Allied Vision Technologies) as described above for contractility analysis. Videos were analyzed in MATLAB using a custom script that calculated the temporal changes in calcium fluorescence intensity. Specifically, each frame was normalized to a baseline background region chosen by the user to give baseline-corrected changes in minimum and maximum fluorescence values for each frame. The temporal change in fluorescence intensity was presented as a calcium transient trace from which the measurements were obtained. Briefly, the calcium transient "timing" was determined as the peak-to-peak values of two successive beats as defined by the peak

maxima. Calcium transient "amplitude" was determined by numerically integrating the area below the peak maxima relative to the baseline. Calcium transient traces were analyzed during 5 mM caffeine stimulation of tissues previously treated with either 1 mM verapamil (Sigma-Aldrich) or 1 μM thapsigargin (Sigma-Aldrich). Caffeine responses were quantified by comparing this calcium transient amplitude before and after the addition of 5 mM caffeine (Sigma-Aldrich).

Conduction velocity

A surrogate of conduction velocity was assessed by calcium propagation within the entire tissues that were pre-treated with 5 μM blebbistatin (Sigma-Aldrich) to uncouple true Ca^{2+}-dependent fluorescent motion from the fluorescent signals caused by motion artifacts. The conduction velocity was calculated by selecting two sections of the tissue within the region of calcium transient propagation and dividing the distance between the centers of these regions by the difference between their peak maxima.

Direct measurements of force

The force generation was measured directly, using an organ bath with high-sensitivity force transducers. Cardiac tissues and FCT strips were transferred to a commercial organ bath system (DMT Myograph) containing oxygenated modified Tyrode's solution (129mM NaCl, 5mM KCl, 2mM $CaCl_2$, 1mM $MgCl_2$, 30mM Glucose, 25mM HEPES, pH 7.4) supplemented with 2% B27 and maintained at a constant temperature of 37°C without electrical stimulation. All measurements were done using LabChart software (ADInstruments). The tissues were allowed to equilibrate for 15 minutes and any spontaneous beating measurements were recorded. The tissues were then allowed to equilibrate for another 15 minutes under electrical stimulation (2 Hz, 5 ms, 80–100 mA, rectangular pulses) in order to preload the tissues by manual stepwise adjustment of the tissue length to that of the maximal force generated, which assumes the optimal sarcomere length is thereby attained.

Twitch tension was measured by increasing the organ bath $[Ca^{2+}] = 0.2 – 2.8$ mmol/L. Specifically, the extracellular calcium concentration was changed by changing the concentration of $CaCl_2$ used in the Tyrode's solution. The tissues were subjected to electrical stimulation for 3 minutes, and an average of 10 contractions were measured. The stimulation was then discontinued for 10, 20, or 30 seconds, and the tissues were allowed to recover for 2 minutes. Post-rest potentiation measurements were subsequently obtained by analyzing the change in twitch tension from the first beat upon re-initiation of electrical stimulation.

Contractility and twitch parameters were further investigated in response to the increasing electrical stimulation frequency within the organ bath as previously described[29]. Twitch forces were calculated as the average of the difference between cyclic peak maximum and minimum force and normalized to the cross-sectional area (obtained by measurement of tissue at the center after force measurements). The force frequency relationship was measured by increasing the electrical stimulation frequency from 1 Hz to 6 Hz at 1 Hz intervals. The tissues were subjected to each stimulation frequency for 30 seconds before

increasing to the following stimulation frequency. The force data were measured at frequencies of 1–6 Hz (in 1 Hz increments) for all experimental groups (static, constant and intensity trained tissues made using early and late iPS-CMs, and human fetal tissue strips) and all iPS cell lines.

Continuous recordings of force and calcium as a function of frequency

Continuous videos were recorded at a rate of 100 frames per second on Zyla 4.2 sCMOS camera (Andor) to determine calcium transients and tissue displacement. The stimulation frequency was increased by 1 Hz every 20 seconds (i.e., every 2,000 frames) from 1–6Hz. The calcium transients were analyzed using custom MATLAB software as described above for measurements of calcium traces, and normalized to the baseline at each frequency as $F-F_0/F_0$. Tissue displacement was measured using the Spottracker module in ImageJ. The areas within the tissue were manually selected at baseline and tracked frame to frame to measure changes in the pixel displacement over time. Calcium dye loading was performed as previously described, but without the use of Blebbistatin to block contractile motion. This enabled measurements of both calcium transient intensity and displacement during calcium imaging.

Immunofluorescent staining

For morphological analysis, tissues and FCTs were fixed by using gradually increasing concentrations of paraformaldehyde (1–4%, in 1% intervals, 1 hour each). Whole tissues were paraffin embedded and cut into 5 μm thick sections. The sectioned tissues were quenched in 0.5M NH_4Cl for 30 minutes, permeabilized with 0.2% Triton X-100 in PBS for 15 minutes and then incubated in blocking solution (1% bovine serum albumin [BSA], 2% goat serum in PBS) for 2 hours. The following primary antibodies were incubated for 2 hours in 1% BSA: anti-sarcomeric α-actinin (1:200, Abcam, ab9465), anti–cardiac troponin T (cTnT, 1:100, Thermo Scientific; MS-295-P1), anti-ryanodine receptor 2 (1:100, Abcam, ab2827), anti-Cav1.2 1:200, Abcam, ab58552), anti-BIN1 (1:100, Abcam, ab137459), anti-mitochondria (1:50, Abcam, ab3298), anti-OXPHOS (1:100, Acris, MS601-720), actin (Alexa Fluor® 350 Phalloidin, Thermo Fisher, A22281).

Tissues were washed 3 times for 5 minutes in 0.2% Triton X-100 and incubated with the corresponding secondary antibodies for 2 hours: anti-mouse–Alexa Fluor 488 (1:400, Invitrogen, A21202), anti-rabbit–Alexa Fluor 568 (1:400, Invitrogen, 81-6114), anti-mouse Alexa Fluor 635 (1:400, Invitrogen, A31574). The tissues were washed and subsequently incubated with NucBlue (Molecular Probes, R37606) for nuclei counterstaining. The immunostained tissues were visualized using a confocal microscope (Olympus Fluoview FV1000).

For t-tubule immunostaining, the tissues were incubated with Wheat Germ Agglutinin (WGA) fluorescently conjugated to Alexa Fluor 488 (Life Technologies, W11261) or di-8-ANEPPS (Life Technologies, D-3167) for 20 minutes before permeabilization and subsequent staining with additional antibodies as described above.

Transmission electron microscopy

Tissues, FCTs, and adult heart tissue were fixed with 2.5% glutaraldehyde in 0.1M Sorenson's buffer (pH 7.2) for 1 hour and sent to the Electron Microscopy and Histology (EM&H Core) Facility at Weill Cornell Medical College for subsequent sample preparation, imaging, and data interpretation in a blinded fashion. Samples were post-fixed for an additional hour with 1% OsO_4 in Sorenson's buffer. After dehydration, the samples were embedded, sectioned, stained with Toluidine Blue and examined under a JEM-1400 electron microscope.

Fraction of cells containing sarcomeres

Sectioned tissues were immunoflourescently labeled with sarcomeric α-actinin and DAPI. Using the cell counter plugin in ImageJ, the DAPI positive cells were marked and counted. Subsequently, all DAPI positive cells that stained positive for α-actinin counted, and the % of cells containing sarcomeres of DAPI positive cells was calculated.

Sarcomere length

Sarcomere length was determined in dissociated cells replated as a monolayer and stained with sarcomeric α-actinin, using a previously published method[9], by measuring the distance between intensity peaks along the long axis of designated cell areas containing clear striations. A minimum of 3 sarcomere lengths per cell were obtained in large numbers of cells from n>6 biological replicates.

Change in tissue area

The change in the projected tissue area (percent change between the contracted and relaxed state) was experimentally determined in bright light by analyzing the change tissues paced at 1 Hz and twice the excitation threshold, by custom-designed MATLAB code that utilized video edge-detection based on the contrast between the darker tissue and the lighter surrounding area. For each group and time point, the change in area was normalized to the change in area measured at Day 6, immediately before the application of electrical stimulation.

Cell morphology

Cells were enzymatically digested using serial digestions of collagenase type 1 and 2 (Worthington), and plated onto 8 well chamber slides (Lab-Tek, Sigma-Aldrich). The cells were allowed to attach for 72hrs and imaged using phase contrast microscopy, Cell area was quantified from these images using the "%Area" function in Image J software after thresholding of the cells in each image. Cell elongation ratio was calculated from these images using the "Roundness" function in Image J where the aspect ratio was defined as (1–Roundness), with 0 corresponding to a circle and 1 corresponding to a completely elongated object[30].

Quantitative PCR

Total RNA was purified from the tissues according to the manufacturer's instructions using TRIzol (Life Technologies). For measurements of adult and FCT NPPA and NPPB

expression, commercial sources were used as follows: adult heart, ages: 30–39, pooled from 3 male hearts TaKaRa/Clontech “Human RNA Mater Panel II”, #636643, Lot#1208462A); fetal hearts, ages: 21–37wk, pooled from 32 male/female fetal hearts (Clontech “Human Fetal Heart Poly A* RNA”, #636156, Lot#7110214, synthesized with oligo dT20 and SSIII kit). Reverse transcription was achieved using Ready-To-Go You-Prime First-Strand Beads (GE Healthcare, 27-9264-01) following manufacturer’s instructions. Genes were quantified by real-time PCR using SYBR Green primers (Life Technologies) and was carried out on Applied Biosystems Step One Plus. Data analysis was carried out using the log 2-fold change normalized to late-stage week 1 tissue gene expression in Fig. 1b, Extended data Fig. 2a. Data analysis was carried out using the fold change normalized to glyceraldehyde-3-phsophate dehydrogenase (GAPDH) gene expression in Extended data Fig. 2b, 9c. The following primers with confirmed integrity that were used can be found in Supplemental Information Primer List.

Oxygen consumption rate and extracellular acidification rate

Engineered cardiac tissues were dissociated into single cells after 4 weeks of cultivation using activated papain solution containing 20 unit/ml papain (~15 min at 37 °C with gentle tapping), as described above for electrophysiological recordings. The enzyme reaction was terminated by FBS (10%) in DMEM/F-12 culture media. The dissociated hiPS-CMs were plated into XF96 Culture Plates (Seahorse Bioscience) coated with Matrigel (Corning, #354230) and cultured for 3 days. Subsequently, the plated hiPS-CMs were assayed in real-time using an XF-96 Extracellular Flux Analyzer (Seahorse Biosciences) for oxygen consumption rate (OCR), and extracellular acidification rate (ECAR) per the manufacturer’s protocols.

Isoproterenol response

Isoproterenol was diluted in standard media (RPMI + B27) to a concentration of 1 μM. Tissues were placed in the organ bath (as previously described), equilibrated for 10 minutes, tissue videos were captured, the force measurements were recorded before and after the addition of the drug, and the change in the generated force was determined.

Patch-clamp electrophysiology

Engineered cardiac tissues were dissociated into single cells for whole-cell patch-clamp recordings at 4 weeks using activated papain solution containing 20 unit/ml papain (Sigma-Aldrich, #76220, from *Caripa papaya*), 1.1mM EDTA, 67uM 2-Mercaptoethanol (Sigma-Aldrich, #M3148), 5.5mM L-Cystein HCl (Sigma-Aldrich, #C7880) in 1x EBSS (Thermo Scientific / Gibco, #24010-043). Particularly, this optimized protocol enabled obtaining healthy patchable single cardiomyocytes without spontaneous beating from early/intensity cardiac tissues. The same dissociation protocol using papain was also used for the other cardiac tissue samples. The tissues were incubated for ~15 min at 37 °C with gentle tapping, and the enzyme reaction was terminated by FBS (10%) in DMEM/F-12 culture medium.

Whole-cell patch-clamp recordings of dissociated iPSC-CMs were conducted using a patch-clamp amplifier (MultiClamp 700B, Molecular Devices) and an inverted microscope equipped with differential interface optics (Nikon, Ti-U). The glass pipettes were prepared

using borosilicate glass (Sutter Instrument, BF150-110-10) and a micropipette puller (Sutter Instrument, Model P-97).

Current-clamp recording for action potential measurement were conducted in normal Tyrode solution containing 140mM NaCl, 5.4mM KCl, 1mM $MgCl_2$, 10mM glucose, 1.8mM $CaCl_2$ and 10mM HEPES (pH7.4 with NaOH at 25 °C) using the pipette solution: 120mM K D-gluconate, 25mM KCl, 4mM MgATP, 2mM NaGTP, 4mM Na_2-phospho-creatin, 10mM EGTA, 1mM $CaCl_2$ and 10mM HEPES (pH 7.4 with KCl at 25 °C). Action potentials were stimulated (5ms, 0.3nA) in a current clamp mode at 37°C (0.2 Hz), recorded and analyzed using Clampfit 10.4 (Axon Instruments).

Voltage-clamp measurements for I_{K1} current recording were conducted using an extracellular solution containing 160mM NMDG, 5.4mM KCl, 2mM $MgCl_2$, 10mM glucose, 10μM nisoldipine, 1μM E-4031 and 10mM HEPES (pH7.2 with HCl at 25 °C) and a pipette solution of 150mM K-gluconate, 5mM EGTA, 1mM MgATP and 10mM HEPES (pH 7.2 with KOH at 25 °C). The following pulse protocols were used: 2-sec long voltage clamp applied from −130 to +10 mV (holding at −40 mV, 0.1 Hz 2-sec voltage pulse). The I_{K1} reversal potential (Ba^{2+}-sensitive current) had a negative slope conductance consistent with inward rectification, as previously described[30]. The current-voltage plot was analyzed before and after the addition of 0.5 mM $BaCl_2$ for 2min.

Dose response curves

Drugs were diluted in standard media (RPMI + B27). Successively higher doses of each drug were administered at concentrations of 10^{-11} M to 10^{-5} M, in decigram increments. Tissue videos were captured ≥ 5 minutes after each dose was administered, and processed using custom image processing software as discussed above. For chronotropic drugs, brightfield videos were taken at each drug concentration so that measurements of the beat frequency could be determined as a function of drug concentration. For ionotropic drugs, tissues were placed in the organ bath and force measurements were recorded as previously described at each drug concentration so that the measurements of the change in force generated could be determined as a function of drug concentration. Dose-response curves for these parameters could be constructed by using MATLAB to fit the Hill Equation for sigmoid curves to the data, to determine the corresponding EC_{50} value.

Paced isoproterenol response

Cardiac tissues were loaded with calcium dye as described above. Tissues were transferred to standard medium (RPMI + B27), paced at 1 Hz for 30 minutes to equilibrate, and the baseline video recordings were then obtained. Successively higher doses of isoproterenol were administered directly to the standard medium at concentrations of 0.01, 100 and 1,000,000 nM. Videos of tissues were captured ≥ 10 min after each dose was administered, and processed using custom-designed image analysis software, as described above.

Cardiac hypertrophy model

Cardiac tissues were exposed to drugs known to induce pathological hypertrophy (angiotensin-II, endothelin-1, isoproterenol) on Day 6 following tissue formation. The first

time point (1 week) was taken after 24 hrs of incubation with or without the drug. The majority of the HCM data shown are from pathologically induced HCM via endothelin-I addition (unless data from all 3 drugs are shown), since the results were comparable amongst the three HCM inducing agents.

Statistics and Reproducibility

Data are shown as the Mean ± 95% CI. Differences between experimental groups were analyzed by one-way or two-way ANOVA. Post-hoc pairwise analysis was done using Tukey's Honest Significant Difference test. Electrophysiological data were analyzed by one-way ANOVA Barlette's test with multiple comparisons. $P < 0.05$ was considered significant for all statistical tests. The reproducibility of the data is demonstrated by the number of independent biological samples and the number of independent experiments performed for each data set within the Main Figures is detailed in the Supplemental Information Main Figure Data Sample Sizes. Details involving the sample sizes used in the Extended Data are included in the figure legends.

Data and protocol availability

Source data are made available for quantitative data shown in all figure panels of the article and can be accessed at DOI 10.6084/m9.figshare.5765559. The study used a combination of commercial and open-source software packages, which are specified in the Methods section, and the custom-designed software that will be available to interested investigators. There are no restrictions to data availability. Detailed experimental protocol is available from the Nature Protocol Exchange and can be accessed at **DOI** 10.1038/protex.2018.030.

Extended Data

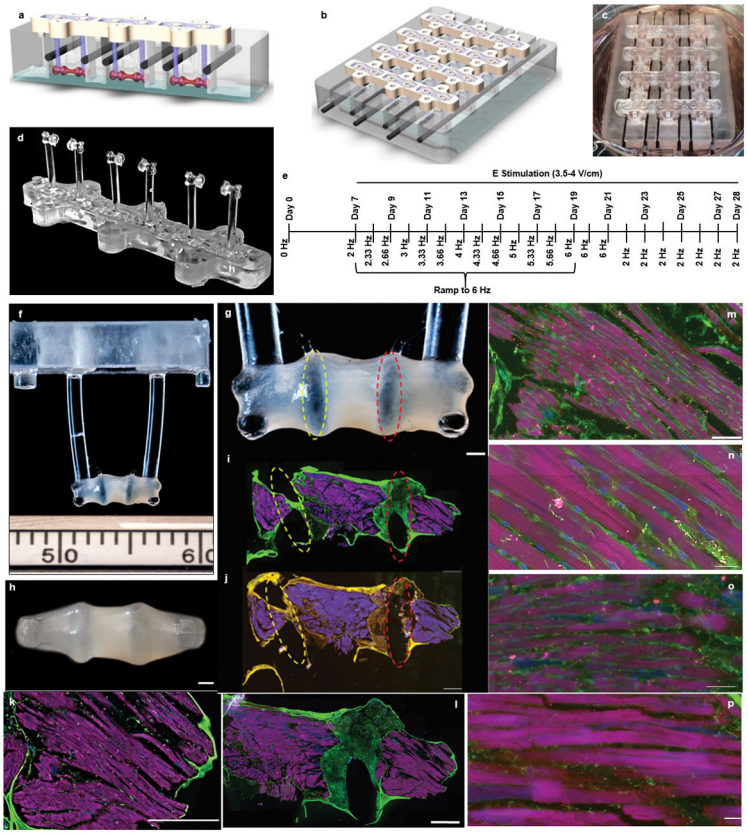

Extended Data Figure 1. Experimental design and the overall appearance of cardiac tissues

a A schematic of the pillars (purple) placed via interlocking mating components between the bioreactor wells (gray) and pillar lid (yellow) with tissues (pink) formed around the pillars, and electrodes (black) placed perpendicular to the cardiac tissues. A glass slide (blue) is epoxied to the bottom of the bioreactor to enable facile video acquisition. **b** A schematic of the assembled bioreactor. **c** Photographs of the cardiac tissues cultured within the bioreactor. **d** The tissue pillar. **e** Increase in the electrical stimulation frequency throughout the intensity training regimen. Photographs of the tissues attached to pillars at the end of 4-week cultivation: **f–g** Side view. **h** Bottom view. Scale bars: 500 μm. **g–j** Serial immunofluorescent sections of the early stage intensity trained tissue with dotted yellow and red lines indicating corresponding pillar placement within tissue. Scale bars: 500 μm. **k–p** Serial immunofluorescent sections of the early stage intensity trained tissue photographed in **i** at four different magnifications from different regions. WGA: green; alpha-actinin: pink; nuclei: blue. Scale bars: (**i–l**) 500 μm, **m** 100 μm, **n** 20 μm, **o–p** 50 μm. Images were selected to include landmark features that facilitate localization and comparisons. Similar results were obtained from 3 independent experiments.

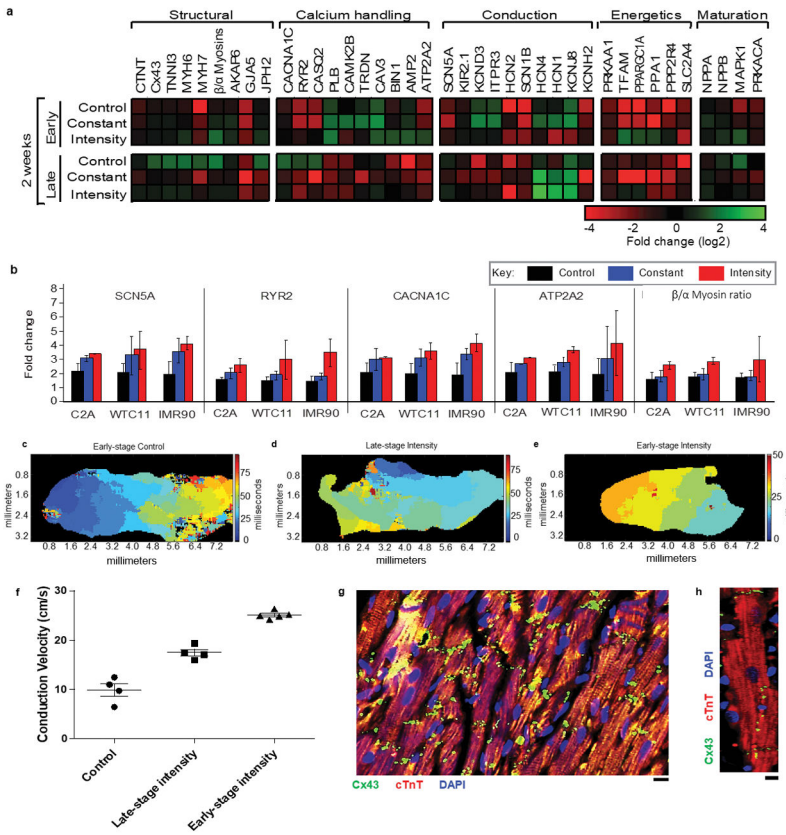

Extended Data Figure 2. Enhanced gene expression and conduction within intensity trained cardiac tissues over time

a Quantitative gene expression of FCTs and C2A hiPS cardiac tissues as determined by qPCR after 2 weeks of culture, fold change relative to late-stage tissues at the start of stimulation. **b** Quantitative gene expression of early-stage cardiac tissues, normalized to GAPDH, from 3 different hiPS lines as determined by qPCR after 4 weeks of culture. n = 12 biologically independent samples per group, Mean ± 95% CI, no significance at $p<0.05$ between different cell lines by 2-way ANOVA. **c–f** Representative conduction velocity activation maps for **c** early-stage control, **d** late-stage intensity, and **e** early-stage intensity trained cardiac tissues and **f** Surrogate of conduction velocity within early- and late-stage C2A hiPS cardiac tissues after 4 weeks of culture, assessed by calcium propagation. Mean ± SEM, n=4–5 biologically independent samples per group. **g–h** Representative immunofluorescent images of gap junction (Connexin-43 (Cx43), green) expression within early-stage intensity-trained hiPS cardiac tissue (cardiac troponin T (cTnT), red), nuclei (DAPI, blue)) after 4 weeks of culture at **g,** lo magnification (scale bar = 10 μm) and **h** high magnification (scale bar = 5 μm). Similar results were obtained from 4 independent experiments.

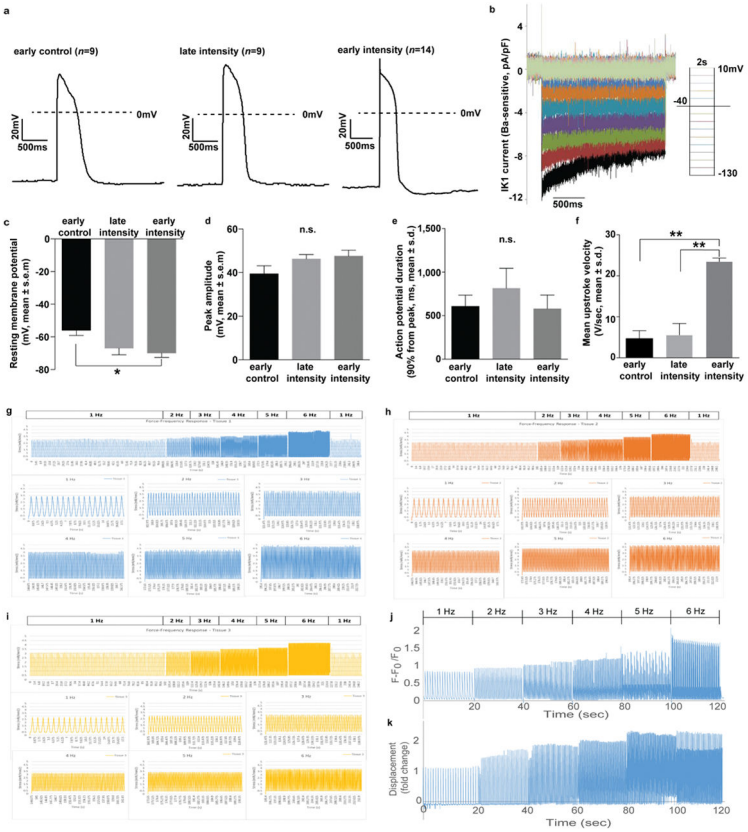

Extended Data Figure 3. Electrophysiological characterization of human engineered cardiomyocytes

a Representative traces of action potentials in early control (n=9), late intensity (n=9) and early intensity (n=14) groups, where n is biologically independent sample obtained during 2 independent experiments. **b** Representative traces of IK1 current for early intensity group using voltage clamp mode. **c–f** Electrophysiological data after 4 weeks of culture detailing the **c** Resting membrane potentials, **d** Peak amplitude, **e** Action potential duration and **f** Upstroke velocity obtained during 2 independent experiments resulting in biologically independent data from early control (n=9), late intensity (n=9) and early intensity (n=14) groups. **P<0.01, *P<0.05 using One-way ANOVA Barlette's test with multiple comparison, n.s.=not significant. **g–i** Representative continuous organ bath force recordings under electrical pacing from 1–6 Hz from three biologically independent early-stage intensity trained tissues (C2A cells) during one experiment. **j–k** Representative continuous recordings from an early-stage intensity trained tissue (C2A cells) under electrical pacing from 1–6 Hz of **j** calcium and k surrogate force as determined by tissue displacement normalized to 1 Hz.

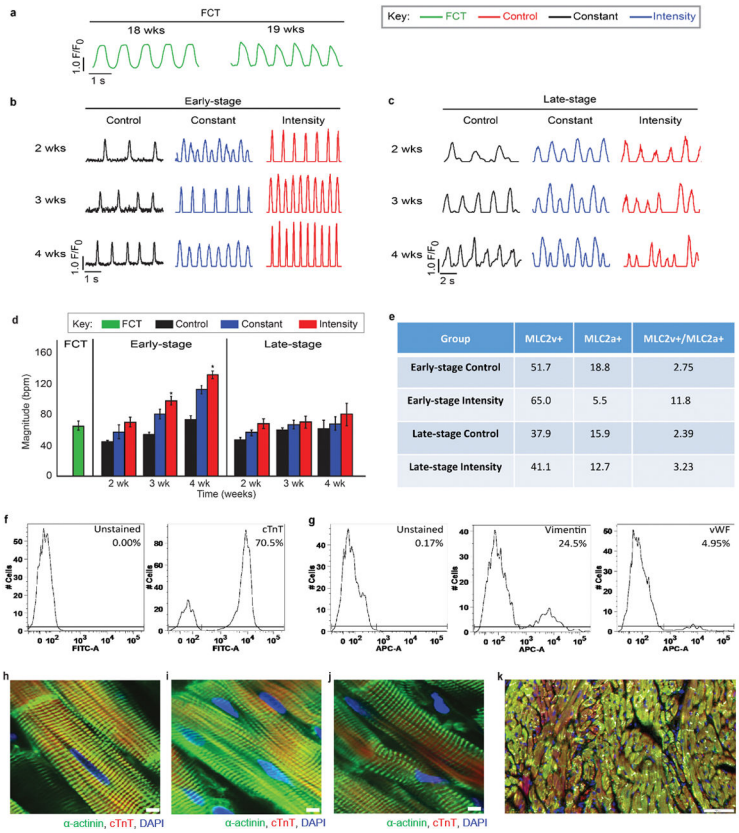

Group	MLC2v+	MLC2a+	MLC2v+/MLC2a+
Early-stage Control	51.7	18.8	2.75
Early-stage Intensity	65.0	5.5	11.8
Late-stage Control	37.9	15.9	2.39
Late-stage Intensity	41.1	12.7	3.23

Extended Data Figure 4. Enhanced maturation and synchronicity of cardiac tissues in response to training regimen as a function of time

Representative contraction profiles of **a** fetal cardiac tissues (FCT), **b** early-stage and **c** late-stage cardiac tissues (C2A cell line) over time. **d** Frequency of contractions in cardiac tissues over 4 weeks of culture (n = 35 biologically independent samples over 16 independent experiments) Mean ± 95% CI, *p<0.05 compared to control group by two-way ANOVA with Tukey's HSD test. Early-stage intensity training is significant against other training regimens by two-way ANOVA with Tukey's HSD test**. e** Characterization of cardiac cell population within cardiac tissues (C2A line) after 4 weeks of culture by FACS analysis. Characterization of cells isolated from early-stage intensity trained cardiac tissues (C2A line) by FACS analysis after 4 weeks of culture for **f** cardiac cells (cardiac troponin T, cTnT) and **g** supporting fibroblast cells (vimentin) and endothelial cells (von Willebrand Factor, vWF). **h**–**j** Representative immunofluorescent images obtained from whole tissues via confocal microscopy detailing the enhanced cardiac ultrastructure: a-actinin (green), cardiac troponin T (red), nuclei (blue) within early-stage cardiac tissues from the **h** C2A line, **i** WTC11 cell line, and **j,** IMR90 cell line after 4 weeks of culture (scale bar = 5 μm, experiment repeated independently 14 times with similar results). **k** Representative immunofluorescent images detailing the cell population: cardiac troponin T (cTnT, green), vimentin (red), nuclei (blue) within a histological section from early-stage cardiac tissue (C2A line) after 4 weeks of culture (scale bar = 50 μm, experiment repeated independently 2 times with similar results).

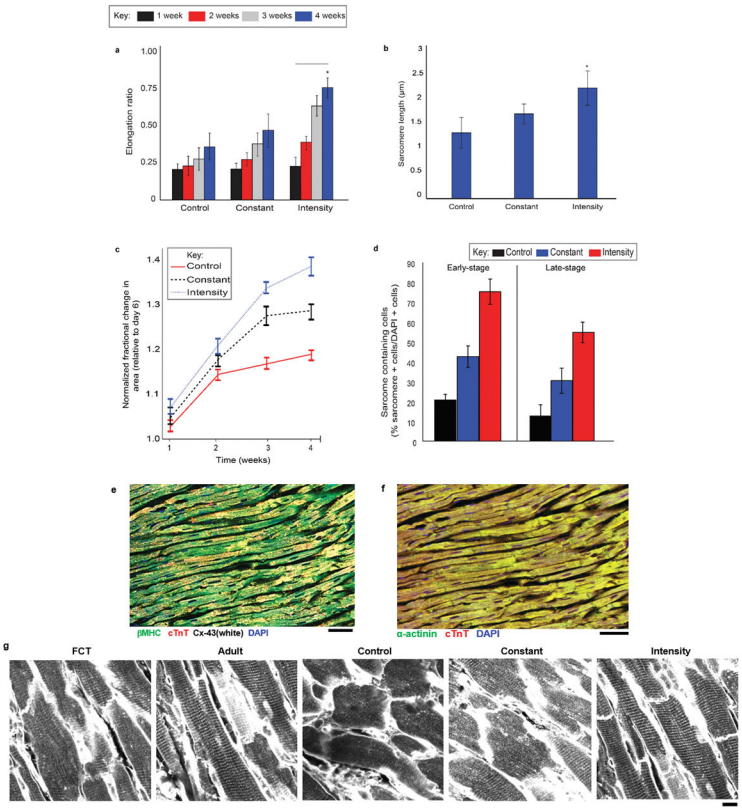

Extended Data Figure 5. Physiological hypertrophy within cardiac tissues enhances contractility

Physiological hypertrophy of CM's cultured within the electromechanically conditioned cardiac tissue format increases as a function of time and training regimen beyond FCT levels**,** as detailed by **a** cell elongation ratio and **b** sarcomere length (n=326 biological replicates from 15 independent samples during one independent experiment). **c** This enables the change in area while being electrically paced at 1 Hz, an indirect measure of fractional shortening, to similarly increase beyond FCT levels as a function of time and training regimen. Data represent the ratio of the change in area for a given time point and the change in area at day 6; n=6 biologically independent samples per group, Mean ± 95% CI, * = $p<0.05$ compared to FCT group at week 4 by ANOVA with Tukey's HSD test and — = $p<0.05$ compared to other training regimens by 2-way ANOVA with Tukey's HSD test). The enhanced cardiac ultrastructure within intensity trained early-stage cardiac tissues is documented by the **d** quantification of sarcomere distribution within cardiac tissues (n=12 biologically independent samples per group, Mean ± 95% CI), Representative immunofluorescent images of **e** gap junction (Connexin-43 (Cx43), white) expression within early-stage hiPS cardiac tissue (b-Myosin heavy chain (**b**MHC, green), cardiac troponin T (cTnT, red), nuclei (DAPI, blue)) and **f** cardiac ultrastructure within early-stage hiPS cardiac tissue (**a**-actinin, green), cardiac troponin T (cTnT, red), nuclei (DAPI, blue)) after 4 weeks of culture (scale bar: 50 μm, experiment repeated independently 3 times with similar results) and **g** immunofluorescent images of α–actinin (white) within cardiac tissues after 4 weeks of culture (scale bar = 10 μm, experiment repeated independently 2 times with similar results).

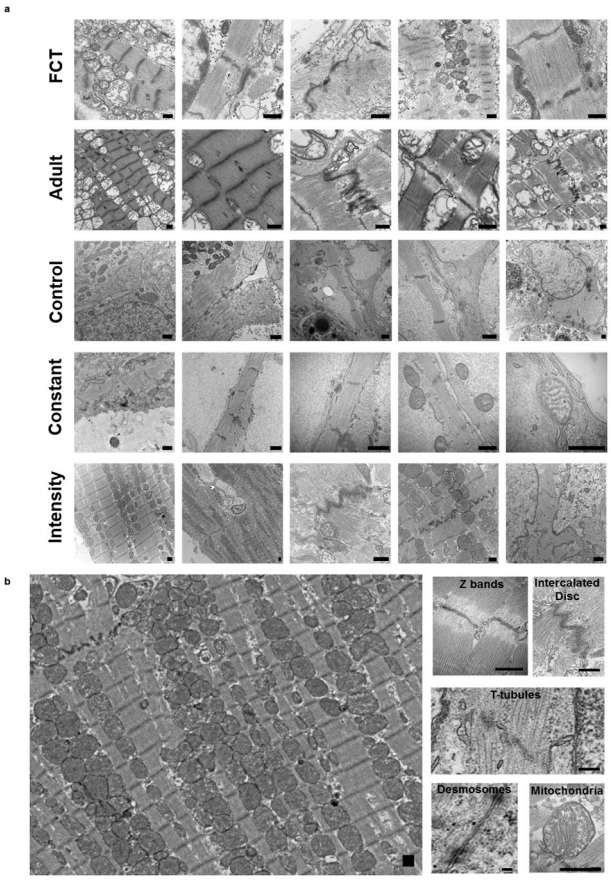

Extended Data Figure 6. Enhanced ultrastructural properties of cardiac tissues via intensity training

a Representative TEM images for FCTs, adult cardiac tissue, and early-stage cardiac tissues (C2A line) using different electromechanical conditioning regimens after 4 weeks of culture (scale bar = 500 nm). **b** TEM images of intensity trained early-stage cardiac tissues (C2A line) after 4 weeks of culture detailing various ultrastructural elements (scale bar: 500 nm). Similar results to those in **a**–**b** were obtained independently as follows: FCT (n=8), Adult (n=2), Control (n=3), Constant (n=3), Intensity (n=4).

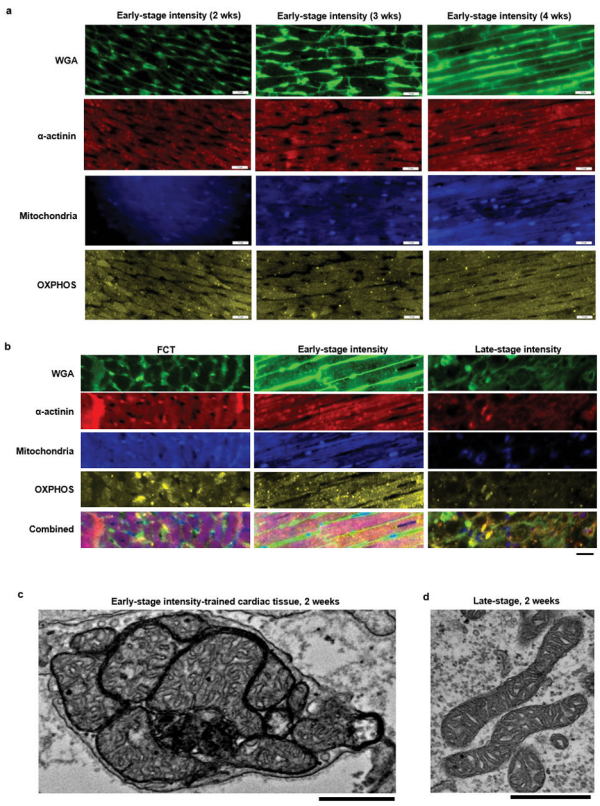

Extended Data Figure 7. Intensity training of early-stage cardiac tissues is required to enhance mitochondrial development

a Representative immunofluorescent images detailing various ultrastructural proteins (WGA (green), α-actinin (red), mitochondria (blue), oxidative phosphorylation (yellow)) for early-stage cardiac tissues (C2A cell line) at different culture times during exposure to the intensity training electromechanical conditioning regimen (scale bar: 20 μm). **b** Representative immunofluorescent images detailing ultrastructural proteins (WGA (green), α-actinin (red), mitochondria (blue), oxidative phosphorylation (yellow)) of cardiac tissues cultured under intensity training for 4 weeks from early-stage hiPS-CMs (C2A cell line), late-stage hiPS-CMs (C2A cell line), and 19 week old fetal cardiac tissue (FCT) (scale bar: 20 μm). Similar results to those in **a**–**b** were obtained independently as follows: FCT (n=5), Early-stage intensityl (n=3), Late-stage intensity (n=3). **c**–**d** Representative TEM images for **c,** early-stage and **d,** late-stage cardiac tissues (C2A cell line) after 2 weeks of exposure to the intensity training electromechanical conditioning regimen (scale bar: 1 μm, experiment not repeated independently).

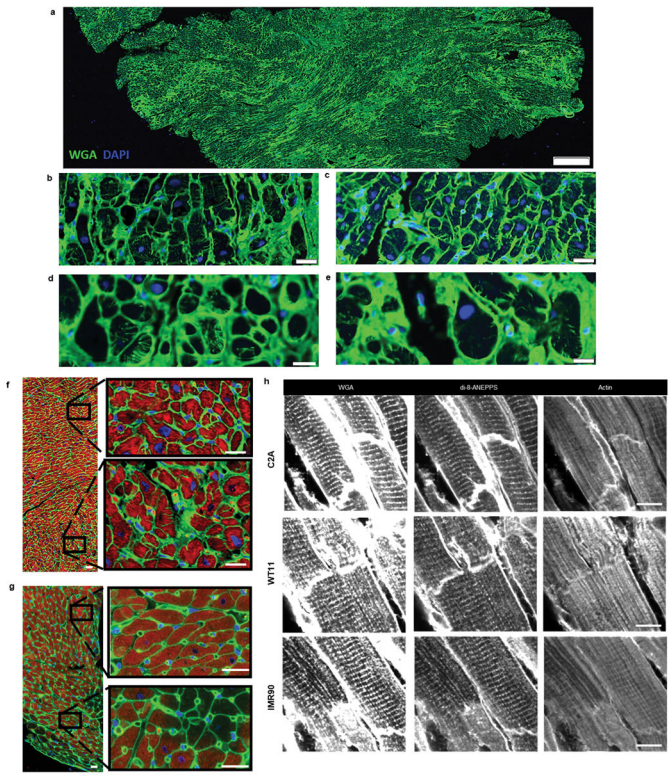

Extended Data Figure 8. Formation of T-tubules within early-stage intensity trained cardiac tissues

a Axial tissue cross sections from intensity trained cardiac tissues (C2A line) after 4 weeks of culture detailing t-tubules, as stained with WGA (green), and nuclei, as stained with DAPI (blue) at **a** low magnification (scale bar: 100 μm), **b**–**c** medium magnification (scale bar: 10 μm) and **d**–**e** high magnification (scale bar: 5 μm), **f**–**g** Axial tissue cross sections detailing t-tubules (as stained with WGA (green), actin (red) and DAPI (blue)) within **f** intensity trained cardiac tissues (C2A line) after 4 weeks of culture and **g** 19 week old FCT. (scale bar: 10 μm). **h** Immunofluorescent stains of paraffin embedded and sectioned cardiac tissues from 3 different hiPS cell lines (C2A, WT11, IMR90) after 4 weeks of intensity training detailing the formation of T-tubules (confirmed by both WGA staining and di-8-ANEPPS staining), and striated ultrastructure (actin) (scale bar: 10 μm). Similar results to those in **a**–**h** were obtained independently in a minimum of 4 independent experiments.

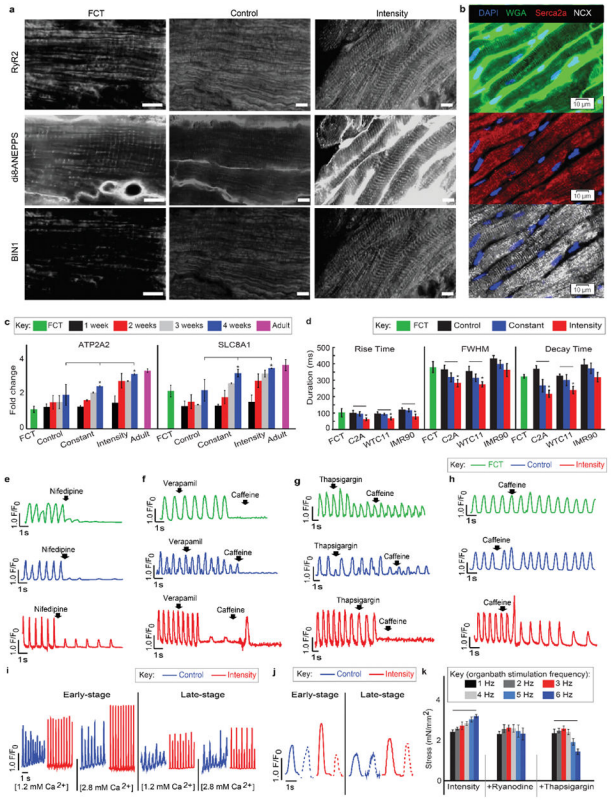

Extended Data Figure 9. Intensity training upregulates cardiac maturation within early-stage tissues through enhanced calcium handling

a,b Intensity training promotes t-tubule formation within early-stage hiPS-CM tissues as demonstrated by immunofluorescence imaging of ryanodine 2 receptor (RyR2, green), di-8-ANEPPs/t-tubules (red), and bridging integrator 1 (BIN1, blue) (scale bar = 10 μm). **c** Gene expression, normalized to GAPDH, of (i) ATP2A2 and (ii) SLC8A1, responsible for maintaining proper calcium homeostasis, within early-stage tissues as determined by qPCR over 4 weeks of culture for the designated stimulation regimen (independent biological replicates per group: FCT (n=8), Control/Constant (n=6), Intensity (n=14), Adult (n=1)), Mean ± 95% CI, *p<0.05 versus FCT group at week 4 by ANOVA with Tukey's HSD test and —p<0.05 compared to other training regimens by 2-way ANOVA with Tukey's HSD test. **d** Relaxation times within early-stage tissues as characterized by the Full-Width Half-Max (FWHM) values and the Decay Time (90% of the time from the maximal peak of the calcium transient). Independent biological replicates per group: FCT (n=8), C2A (n=12), WTC11 (n=6), IMR90 (n=6). Mean± 95% CI, *p<0.05 versus FCT group by ANOVA with Tukey's HSD and — p<0.05 between cell lines by two-way ANOVA). **e** Representative calcium traces of early-stage tissues treated with 1 μM nifedipine**. f–g** Representative traces of calcium release after stimulation with 5mM caffeine in early-stage tissues and FCTs treated with **f** 1 mM verapamil or **g** 2 μM thapsigargin. **h** Representative traces of calcium release after stimulation with 5 mM caffeine for early-stage tissues and FCTs. **i** Calcium spikes (by immunofluorescent calcium dyes) in early and late-stage tissues (C2A line) after 4 weeks of culture at two [Ca2+] levels. **j** Intensity-trained early-stage but not late-stage tissues (C2A line) after 4 weeks of culture respond to ryanodine (1μmol/L). **k** The force-

frequency relationship of early-stage intensity-trained cardiac tissues (C2A line) after 4 weeks of culture treated with the ryranodine blocker ryanodine (1μM) or the SERCA2a blocker thapsigargin (1μM) (directly measured force data, n=13 biologically independent samples for Intensity group and n=3 biologically independent samples for other groups), Mean ± 95% CI, —P<0.05 by two-way ANOVA.

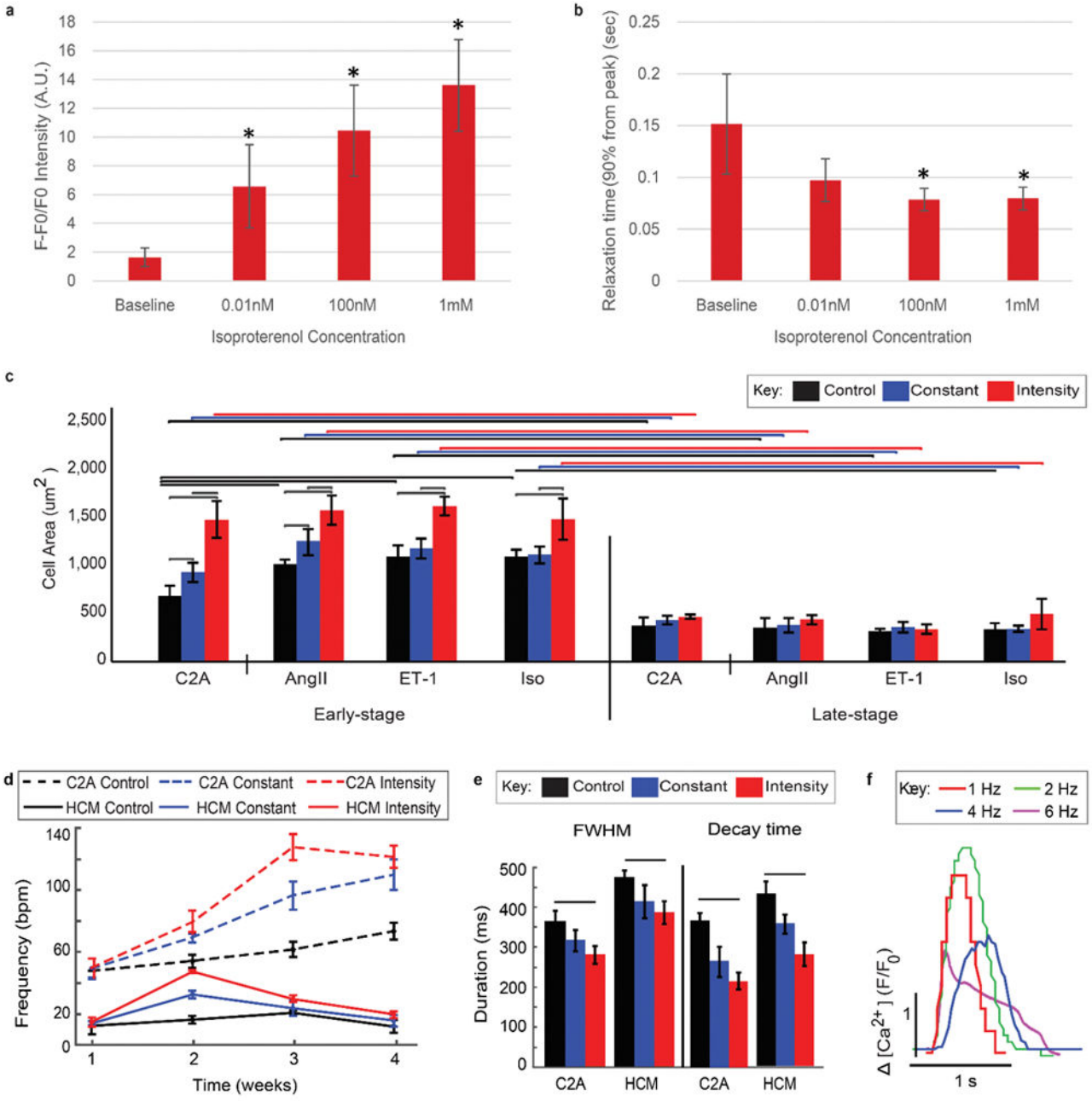

Extended Data Figure 10. Intensity training within early-stage tissues enables physiologically relevant drug responses and the development of a pathological hypertrophy disease model

a Calcium intensity measurements and **b** Relaxation time obtained by measuring the time from the peak to 90% of the relaxation (R90) during electrical pacing at 1 Hz within early-

stage intensity trained tissues (C2A line) after 4 weeks of culture for increasing doses of Isoproterenol. n = 20 biological replicates from 6 independent experiments. Mean ± 95% CI, * $p<0.05$ versus baseline response by ANOVA with Tukey's HSD test. **c** Cell Area over 4 weeks of culture for the designated stimulation regimen. n = 10 biological replicates from 5 independent experiments. Mean ± 95% CI, lines: $p<0.05$ compared to other training regimens by 2-way ANOVA with Tukey's HSD test. **d** Frequency of contractions in healthy (C2A) and hypertrophic (HCM) heart tissues over 4 weeks of culture. n = 12 independent biological samples from 5 independent experiments, Mean ± 95% CI. **e** Relaxation times within early-stage tissues (C2A line) and early stage hypertrophy tissues (HCM) as characterized by the Full-Width Half-Max (FWHM) values and the Decay Time (90% of the time from the maximal peak of the calcium transient). n = 20 biological replicates from 4 independent experiments, Mean ± 95% CI; lines: $p<0.05$ compared to other training regimens by 2-way ANOVA with Tukey's HSD test. **f** Early-stage intensity trained hypertrophy tissues demonstrate impaired frequency-dependent acceleration of relaxation (FDAR), as shown for each stimulation frequency by individual traces of calcium peaks.

Supplementary Material

Refer to Web version on PubMed Central for supplementary material.

Acknowledgments

The authors gratefully acknowledge funding support by the National Institute of Health of the USA (NIBIB and NCATS grant EB17103 (GVN); NIBIB, NCATS, NIAMS, NIDCR and NIEHS, grant EB025765 (GVN); NHLBI grants HL076485 (GVN) and HL138486 (MY); Columbia University MD/PhD program (SPM, TC), University of Minho MD/PhD program (DT), Japan Society for the Promotion of Science fellowship (KM), and Columbia University Stem Cell Initiative (DS, LJS, MY). We thank S. Duncan (Medical College of Wisconsin) and B. Conklin (Gladstone Institute and University of San Francisco) for providing human iPS cells, M.B. Bouchard for assistance with image and video analysis, and L. Cohen-Gould for the transmission electron microscopy services.

References

1. Bellin M, Marchetto MC, Gage FH, Mummery CL. Induced pluripotent stem cells: the new patient? Nature reviews Molecular cell biology. 2012; 13:713–726. [PubMed: 23034453]
2. Matsa E, Burridge PW, Wu JC. Human stem cells for modeling heart disease and for drug discovery. Science translational medicine. 2014; 6:239ps236.
3. Wang G, McCain ML, Yang L, He A, Pasqualini FS. Modeling the mitochondrial cardiomyopathy of Barth syndrome with induced pluripotent stem cell and heart-on-chip technologies. Nature medicine. 2014; 20:616–623.
4. Yazawa M, et al. Using induced pluripotent stem cells to investigate cardiac phenotypes in Timothy syndrome. Nature. 2011; 471:230–234. [PubMed: 21307850]
5. Yang X, Pabon L, Murry CE. Engineering adolescence: maturation of human pluripotent stem cell-derived cardiomyocytes. Circulation research. 2014; 114:511–523. [PubMed: 24481842]
6. Feric NT, Radisic M. Maturing human pluripotent stem cell-derived cardiomyocytes in human engineered cardiac tissues. Advanced Drug Delivery Reviews. 2016; 96:110–134. [PubMed: 25956564]
7. Domian IJ, et al. Generation of Functional Ventricular Heart Muscle from Mouse Ventricular Progenitor Cells. Science. 2009; 326:426–429. DOI: 10.1126/science.1177350 [PubMed: 19833966]
8. Lundy SD, Zhu WZ, Regnier M, Laflamme MA. Structural and functional maturation of cardiomyocytes derived from human pluripotent stem cells. Stem cells and development. 2013; 22:1991–2002. [PubMed: 23461462]

9. Nunes SS, et al. Biowire: a platform for maturation of human pluripotent stem cell-derived cardiomyocytes. Nat Meth. 2013; 10:781–787.
10. Mannhardt I, et al. Human Engineered Heart Tissue: Analysis of Contractile Force. Stem Cell Reports. 2016; 7:29–42. [PubMed: 27211213]
11. Ribeiro MC, et al. Functional maturation of human pluripotent stem cell derived cardiomyocytes in vitro--correlation between contraction force and electrophysiology. Biomaterials. 2015; 51:138–50. [PubMed: 25771005]
12. Brette F, Orchard C. T-tubule function in mammalian cardiac myocytes. Circulation research. 2003; 92:1182–1192. [PubMed: 12805236]
13. Wiegerinck RF, et al. Force frequency relationship of the human ventricle increases during early postnatal development. Pediatric research. 2009; 65:414–419. [PubMed: 19127223]
14. Lopaschuk GD, Jaswal JS. Energy metabolic phenotype of the cardiomyocyte during development, differentiation, and postnatal maturation. Journal of cardiovascular pharmacology. 2010; 56:130–140. [PubMed: 20505524]
15. Jackman, et al. Dynamic culture yields engineered myocardium with near-adult functional output. Biomaterials. 2016; 111:66–79. [PubMed: 27723557]
16. Radisic M, et al. Functional assembly of engineered myocardium by electrical stimulation of cardiac myocytes cultured on scaffolds. Proceedings of the National Academy of Sciences. 2004; 101:18129–18134.
17. Eng GLB, Protas L, Gagliardi M, Brown K, Kass RS, Keller G, Robinson RB, Vunjak-Novakovic G. Autonomous beating rate adaptation in human stem cell-derived cardiomyocytes. Nature Communications. Jan.2016 ePublished before print.
18. Tulloch NL, et al. Growth of engineered human myocardium with mechanical loading and vascular coculture. Circulation research. 2011; 109:47–59. [PubMed: 21597009]
19. Hasenfuss G, et al. Energetics of isometric force development in control and volume-overload human myocardium. Comparison with animal species. Circulation research. 1991; 68:836–846. [PubMed: 1742869]
20. Porter GA Jr, et al. Bioenergetics, mitochondria, and cardiac myocyte differentiation. Progress in pediatric cardiology. 2011; 31:75–81. [PubMed: 21603067]
21. Chung S, et al. Mitochondrial oxidative metabolism is required for the cardiac differentiation of stem cells. Nature clinical practice Cardiovascular medicine. 2007; 4(Suppl 1):S60–67.
22. Gong G, et al. Parkin-mediated mitophagy directs perinatal cardiac metabolic maturation in mice. Science. 2015; 350:4.
23. Gottlieb RA, Bernstein D. Mitochondria shape cardiac metabolism. Science. 2015; 350:1162–1163. [PubMed: 26785456]
24. Vega RB, Horton JL, Kelly DP. Maintaining ancient organelles: mitochondrial biogenesis and maturation. Circulation research. 2015; 116:1820–1834. [PubMed: 25999422]
25. Sulkin MS, et al. Nanoscale three-dimensional imaging of the human myocyte. Journal of structural biology. 2014; 188:55–60. [PubMed: 25160725]
26. Hong T, et al. Cardiac BIN1 folds T-tubule membrane, controlling ion flux and limiting arrhythmia. Nature medicine. 2014; 20:624–632.
27. Bers DM. Cardiac excitation-contraction coupling. Nature. 2002; 415:198–205. [PubMed: 11805843]
28. Huebsch N, et al. Miniaturized iPS-Cell-Derived Cardiac Muscles for Physiologically Relevant Drug Response Analyses. Sci Rep. 2016; 6:24726. [PubMed: 27095412]
29. Sun, Ryan, Bouchard, Matthew B., Hillman, Elizabeth MC. Splassh: Open Source Software for Camera-Based High-Speed, Multispectral in-Vivo Optical Image Acquisition. Biomedical Optics Express. 2010; 1:385–97. [PubMed: 21258475]
30. Ma J, et al. High purity human-induced pluripotent stem cell-derived cardiomyocytes: electrophysiological properties of action potentials and ionic currents. American Journal of Physiology - Heart and Circulatory Physiology. 2011; 301:H2006–H2017. [PubMed: 21890694]
31. Shadrin, et al. Cardiopatch platform enables maturation and scale up of human pluripotent stem cell-derived engineered heart tissue. Nature Communications. 2017; 28:1825.

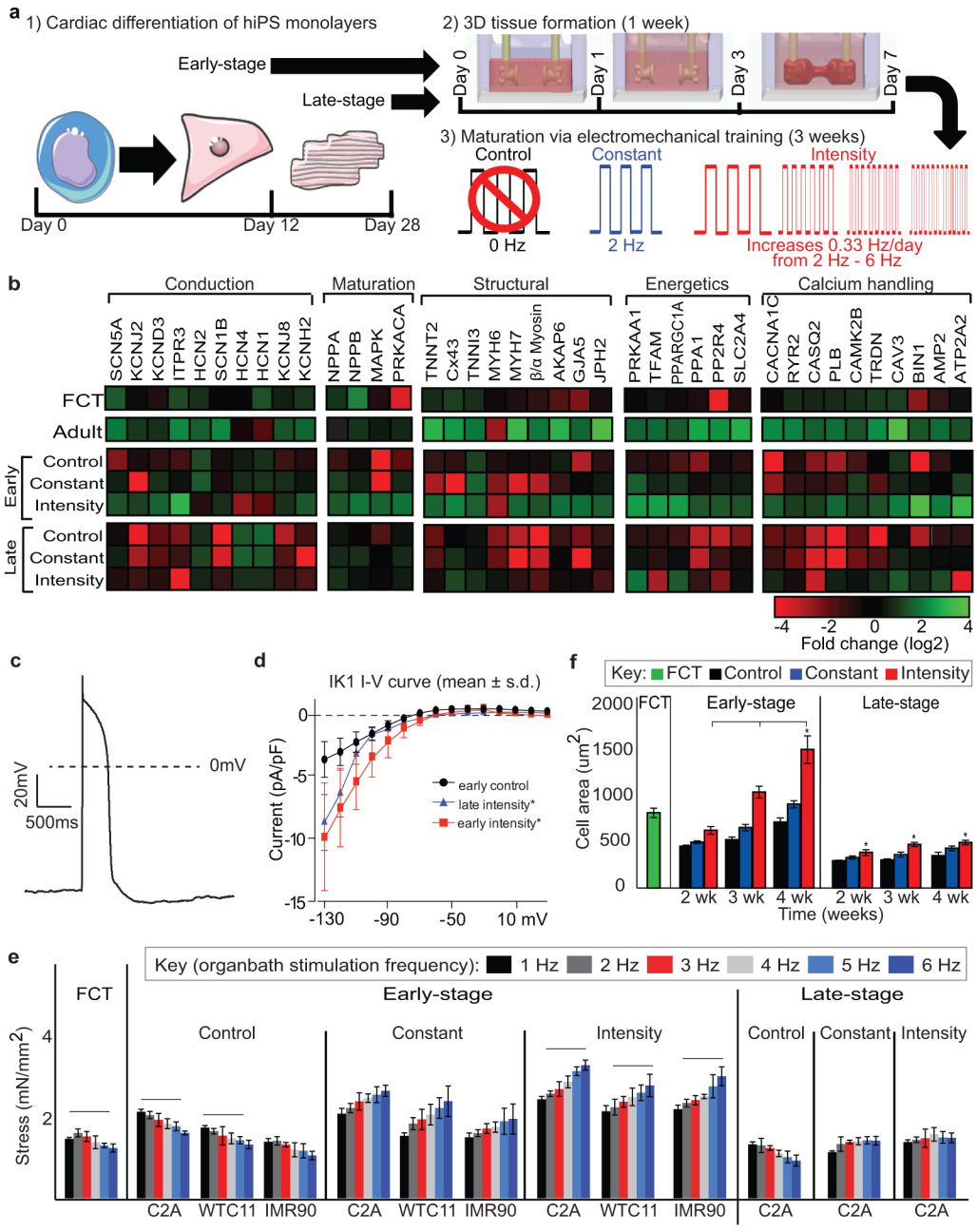

Figure 1. Intensity-training of early-stage cardiac tissues enhances maturation

Data are shown as mean ± 95% CI; sample sizes detailed in SI: Main Figure Data Sample Sizes. **a** Experimental design: early-stage or late-stage iPS-CMs and supporting fibroblasts were encapsulated in fibrin hydrogel to form tissues stretched between two elastic pillars and forced to contract by electrical stimulation. Gradual increase in frequency to supra-physiological levels (intensity regime) was compared to stimulation at constant frequency (constant regime), unstimulated controls, and human adult and fetal heart ventricles. **b** Gene expression data for six groups of cardiac tissues, adult and fetal heart ventricles. **c** Action potential for the *early/intensity* group. d IK1 current-voltage (I–V) curves (mean ± s.d.). **e**

Early/intensity tissues, but not the other groups, developed a positive force-frequency relationship for all three iPS lines (C2A, WTC11, IMR90) after 4 weeks of culture. **f** Cell area over time.

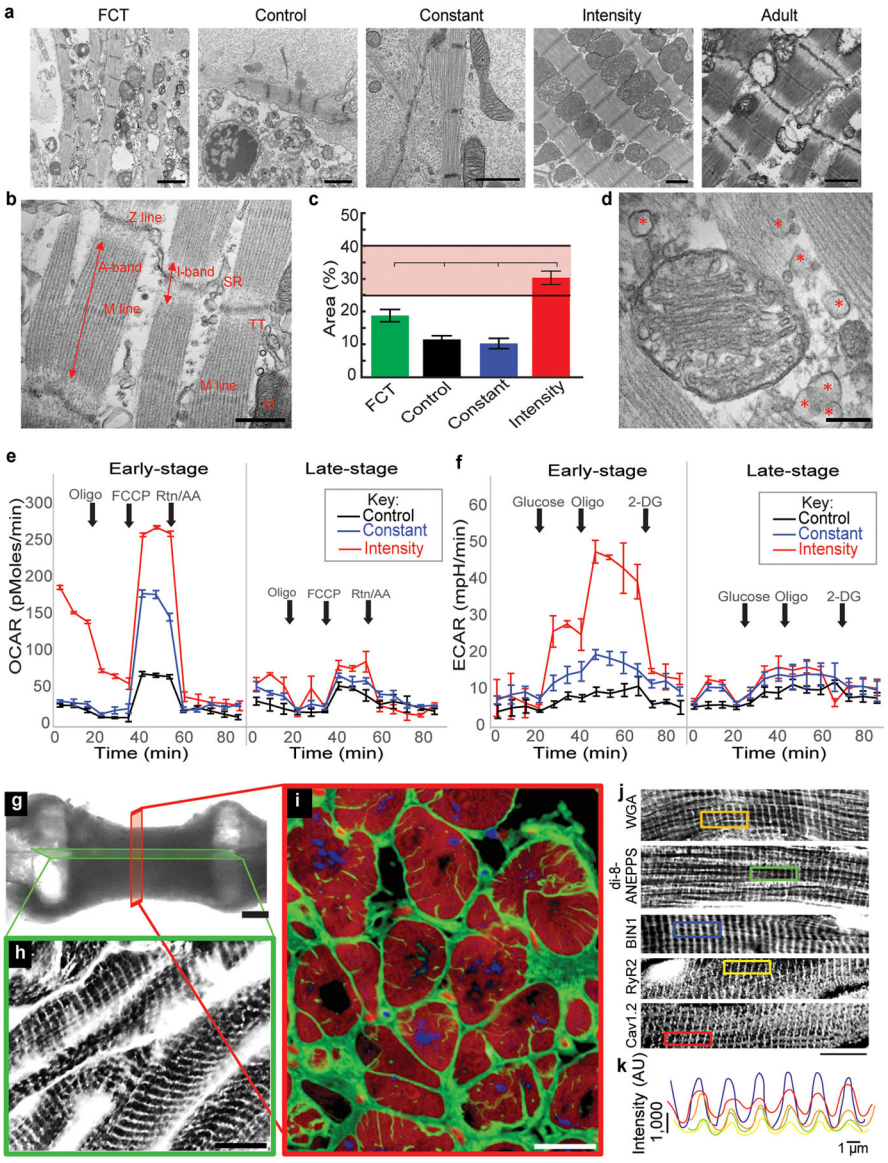

Figure 2. Enhanced cardiac ultrastructure, bioenergetics, and t-tubule formation in *early/intensity* tissues

Data after 4 weeks of culture (C2A cell line) are shown as mean ± 95% CI; sample sizes detailed in SI Main Figure Data Sample Sizes. **a** Transmission electron micrographs (scale bar: 1 µm). **b** Registers of sarcomeres with A- and I-bands, and M- and Z-lines, sarcoplasmic reticulum and t-tubules (scale bar: 1 µm). **c** Density of mitochondria; shaded area represents values from adult human heart. **d** Lipid droplets (red asterisk, scale bar: 1 µm). **e** Oxygen consumption rate. **f** Extracellular acidification rate. **g** Sections taken to evaluate t-tubules (bright field, scale bar: 500 µm). **h–i** t-tubule system (green: WGA; red: cTnT; blue: nuclei; scale bar: 10 µm). **j–k** Calcium handling ultrastructure (scale bar: 15 µm). **k** Regular spacing of calcium handling proteins.

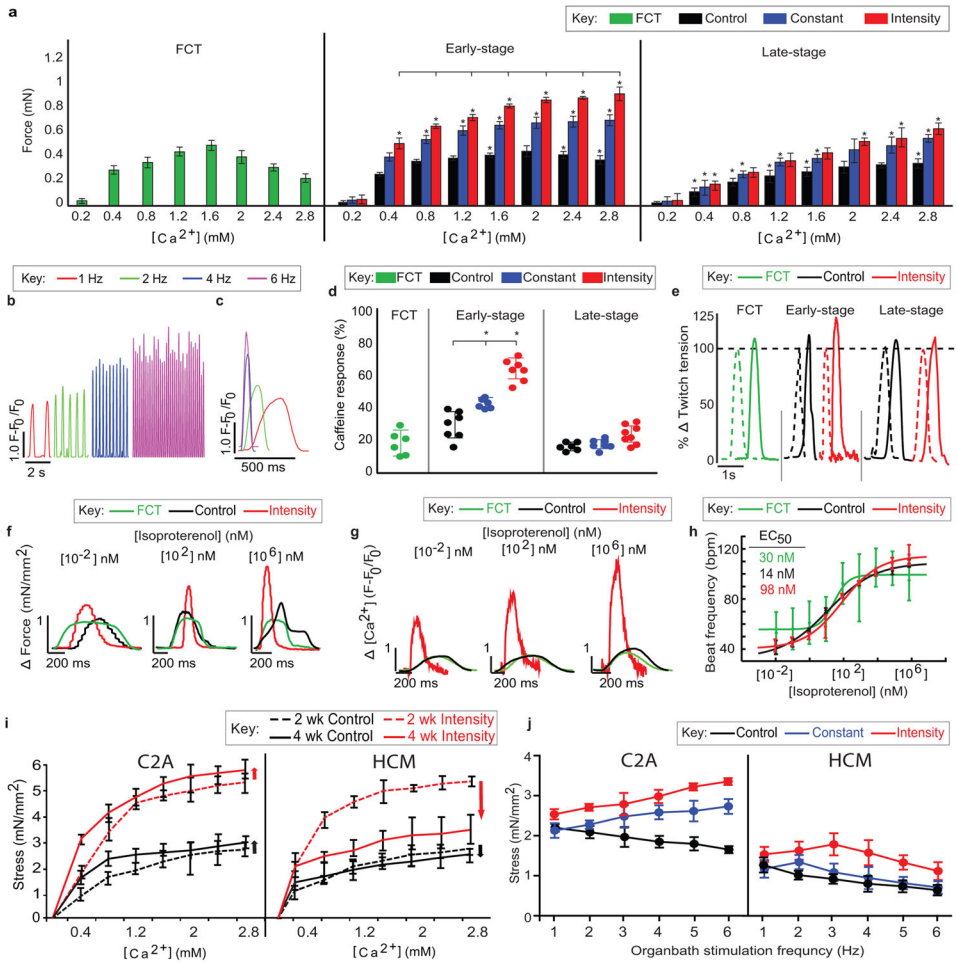

Figure 3. Mature calcium handling in *early/intensity* tissues

Data after 4 weeks of culture (C2A cell line) are shown as mean ± 95% CI; sample sizes detailed in SI Main Figure Data Sample Sizes; * = $p<0.05$ versus FCT using one-way ANOVA followed by Tukey's HSD test; lines = $p<0.05$ versus other training regimens using two-way ANOVA followed by Tukey's HSD test. **a** Force of contraction during the CICR. **b–c** FDAR, shown by traces of calcium. **d** Calcium release after stimulation with 5 mM caffeine. **e** Force traces during post-rest potentiation with 10 seconds of rest. **f** Ionotropic, **g** Lusitropic, and **h** Chronotropic dose-dependent responses. **i**–j Cardiac tissue models of pathological hypertrophy (HCM) reveal **i** decreased CICR over time, and **j** reversal of the positive FFR at higher pacing rates.